

Rotational period of WD1953-011 - a magnetic white dwarf with a star spot

C. S. Brinkworth¹, T. R. Marsh², L. Morales-Rueda³, P. F. L. Maxted⁴,
M. R. Burleigh⁵, S. A. Good⁵

¹ *Department of Physics and Astronomy, University of Southampton, Highfield, Southampton, SO17 1BJ, UK.*

² *Department of Physics, The University of Warwick, Coventry, CV4 7AL, UK.*

³ *Department of Astrophysics, University of Nijmegen, PO Box 9010, 6500GL, Nijmegen, The Netherlands*

⁴ *School of Chemistry and Physics, Keele University, Staffordshire, ST5 5BG, UK*

⁵ *Department of Physics and Astronomy, University of Leicester, Leicester, LE1 7RH, UK.*

18 October 2004

ABSTRACT

WD1953-011 is an isolated, cool ($7920 \pm 200\text{K}$, Bergeron, Legget & Ruiz, 2001) magnetic white dwarf (MWD) with a low average field strength ($\sim 70\text{kG}$, Maxted et al. 2000) and a higher than average mass ($\sim 0.74M_{\odot}$, Bergeron et al. 2001). Spectroscopic observations taken by Maxted et al. 2000 showed variations of equivalent width in the Balmer lines, unusual in a low field white dwarf. Here we present V band photometry of WD1953-011 taken at 7 epochs over a total of 22 months. All of the datasets show a sinusoidal variation of approximately 2% peak-to-peak amplitude. We propose that these variations are due to a star spot on the MWD, analogous to a sunspot, which is affecting the temperature at the surface, and therefore its photometric magnitude. The variations have a best-fit period over the entire 22 months of 1.4418 days, which we interpret as the rotational period of the WD.

Key words: white dwarfs – stars: magnetic fields – stars: individual: WD1953-011 – stars: spots – stars: rotation

1 INTRODUCTION

There are over 120 catalogued isolated magnetic white dwarfs (MWD), comprising $\sim 2\%$ of the total WD population. Their field strengths range from 10kG up to 1000MG (Wickramasinghe & Ferrario, 2000), with temperatures ranging from $\sim 4000\text{K}$ to $>50000\text{K}$. MWDs are important from an evolutionary point of view as they tend to have a higher than average mass than their non-magnetic counterparts, suggesting that the magnetic field affects the initial-to-final mass relationship. They are also extremely useful for determining spin periods, as rotation in non-magnetic white dwarfs is notoriously hard to measure due to the heavy gravitational broadening of their spectral lines. In contrast, a significant fraction of magnetic white dwarfs ($\sim 30\%$) display spectroscopic, spectropolarimetric and/or photometric variability indicative of rotation. Spectral or spectropolarimetric variation is generally believed to be caused by surface field strength variation (e.g. motion of Zeeman-split components of the H Balmer absorption lines), while photometric variability in high-field MWDs is due to the field dependence of the continuum opacity (magnetic dichroism, Ferrario et al.

1997). Low-field MWDs are not expected to show significant photometric variability.

The measured rotational periods of MWDs are unusual as they seem to show a bimodal distribution, with one group rotating very slowly, possibly with periods $> 100\text{years}$, and another group rotating very quickly, of order minutes to hours. This contrasts with the estimates of the rotational periods of non-magnetic WDs, which suggest timescales of ~ 1 day (Heber, Napiwotski & Reid, 1997; O'Brien et al. 1996). These results suggest efficient angular momentum transfer from the core to the envelope and large-scale angular momentum loss during post main-sequence evolution, otherwise WDs should be rotating close to their break-up value. For MWDs, Spruit (1998) proposed that the extremely slow rotators could be produced if the magnetic field locks the forming MWD to its envelope, efficiently shedding angular momentum, while King, Pringle & Wickramasinghe (2001) have suggested that the very fast rotators ($P_{rot} \sim \text{minutes}$) may have been spun up in double-degenerate mergers.

WD1953-011 is a cool ($7920 \pm 200\text{K}$, Bergeron et al. 2001) magnetic white dwarf with a low field strength ($\sim 70\text{kG}$). The field structure of MWDs can usually be mod-

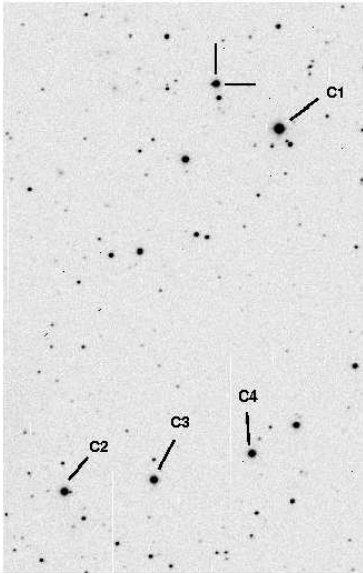


Figure 1. Finding chart for WD1953-011 and the 4 comparison stars used.

elled with a centred or offset dipole, but Maxted et al. (2000) have shown the field structure of WD1953-011 to be more complex, with a strong ($\sim 500\text{kG}$) spot-like field superimposed on a weaker ($\sim 70\text{kG}$) dipolar distribution. Maxted et al. (2000) also discovered changes in the equivalent width of the Balmer lines with time. Here we show that WD1953-011 is also photometrically variable, and we use those variations to find the rotational period of the MWD.

2 OBSERVATIONS

We observed WD1953-011 at 7 epochs between July 2001 and May 2003. In total we obtained 900 observations in the V band. The data were all taken using the 1m Jacobus Kapteyn Telescope on La Palma. A full list of V band observations is given in Table 1, although we also took data in B, R and I broad bands and $H\beta$ narrow band during the July 2001 run. As the results of the photometry were found to be almost identical in all of the bands, we restricted the subsequent observations to V band only. The SITe1 CCD chip is 2088×2120 pixels, with readout noise = 6 e and gain = 1.9 e/ADU. Pixel size is $15\mu\text{m}$ and image scale is $0.33''/\text{pix}$. Fig 1 shows a finding chart for WD1953-011 and the comparison stars.

3 DATA REDUCTION

Each of the seven data sets were reduced in the same way using the packages FIGARO and KAPPA. First the bias frames from a run were combined to form a master bias for the whole run. This was subtracted from all other frames. The flats were then checked, and those with mean counts of less than 7000, or greater than 35000 were discarded. We were concerned that there may be a problem with the flat fields at short exposure times, caused by the shutter speed allowing the centre of the chip to be exposed for a longer

Table 1. List of observations of WD1953-011 taken with the JKT on La Palma. Observers: C S Brinkworth CSB, T R Marsh TRM, L Morales-Rueda LMR, M R Burleigh MRB, S A Good SAG

Dates	Filter	Exp (s)	N	Observer	Conditions
05/07/01	V Kitt	40	14	TRM	Good
06/07/01	V Kitt	40	18	TRM	Fair
07/07/01	V Kitt	40	19	TRM	Superb
08/07/01	V Kitt	40	6	TRM	Poor seeing
09/07/01	V Kitt	40	9	TRM	Good
10/07/01	V Kitt	40	12	TRM	Good
11/07/01	V Kitt	40	12	TRM	Good
14/05/02	V Harris	40	30	MRB,SAG	Cirrus
15/05/02	V Harris	40	45	MRB,SAG	Good
16/05/02	V Harris	40	25	MRB,SAG	Variable
17/05/02	V Harris	40	40	MRB,SAG	Good
26/05/02	V Harris	60	15	TRM,CSB	Good
27/05/02	V Harris	60	10	TRM,CSB	Good
28/05/02	V Harris	60	20	TRM,CSB	Cirrus
29/05/02	V Harris	60	20	TRM,CSB	Cirrus
30/05/02	V Harris	60	30	TRM,CSB	Cirrus
31/05/02	V Harris	60	20	TRM,CSB	Good
01/06/02	V Harris	60	20	TRM,CSB	Good
15/07/02	V Harris	60	26	LMR	Good
16/07/02	V Harris	60	36	LMR	Good
17/07/02	V Harris	60	11	LMR	Good
18/07/02	V Harris	60	25	LMR	Good
19/07/02	V Harris	60	27	LMR	Good
20/07/02	V Harris	60	29	LMR	Good
21/07/02	V Harris	60	34	LMR	Good
02/08/02	V Harris	60	5	MRB,CSB	Good
03/08/02	V Harris	60	20	MRB,CSB	Good
04/08/02	V Harris	60	15	MRB,CSB	Good
05/08/02	V Harris	120	15	MRB,CSB	Some cirrus
06/08/02	V Harris	40	15	MRB,CSB	Superb
07/08/02	V Harris	60	5	MRB,CSB	Good
10/09/02	V Harris	60	30	TRM	Good
11/09/02	V Harris	60	24	TRM	Cirrus
12/09/02	V Harris	60	32	TRM	Superb
13/09/02	V Harris	60	40	TRM	Some cirrus
15/09/02	V Harris	100	20	TRM	Poor seeing
08/05/03	V Harris	60	3	LMR	High cloud
09/05/03	V Harris	60	4	LMR	Good
10/05/03	V Harris	60	5	LMR	Good
11/05/03	V Harris	60	5	LMR	Poor seeing
12/05/03	V Harris	60	5	LMR	Good
13/05/03	V Harris	60	5	LMR	Good
14/05/03	V Harris	60	5	LMR	Good
15/05/03	V Harris	60	5	LMR	Good
16/05/03	V Harris	60	10	LMR	Twilight
17/05/03	V Harris	60	8	LMR	Twilight
18/05/03	V Harris	60	5	LMR	Variable seeing
20/05/03	V Harris	60	6	LMR	High cloud
21/05/03	V Harris	60	5	LMR	Good
22/05/03	V Harris	60	5	LMR	Dusty
23/05/03	V Harris	60	5	LMR	Good
25/05/03	V Harris	60	5	CSB, MRB	Good
26/05/03	V Harris	90	5	CSB, MRB	Superb
27/05/03	V Harris	60	5	CSB, MRB	Superb
28/05/03	V Harris	60	10	CSB, MRB	Clear but dusty
29/05/03	V Harris	60	5	CSB, MRB	Good
30/05/03	V Harris	60	5	CSB, MRB	Good
31/05/03	V Harris	60	10	CSB, MRB	Superb

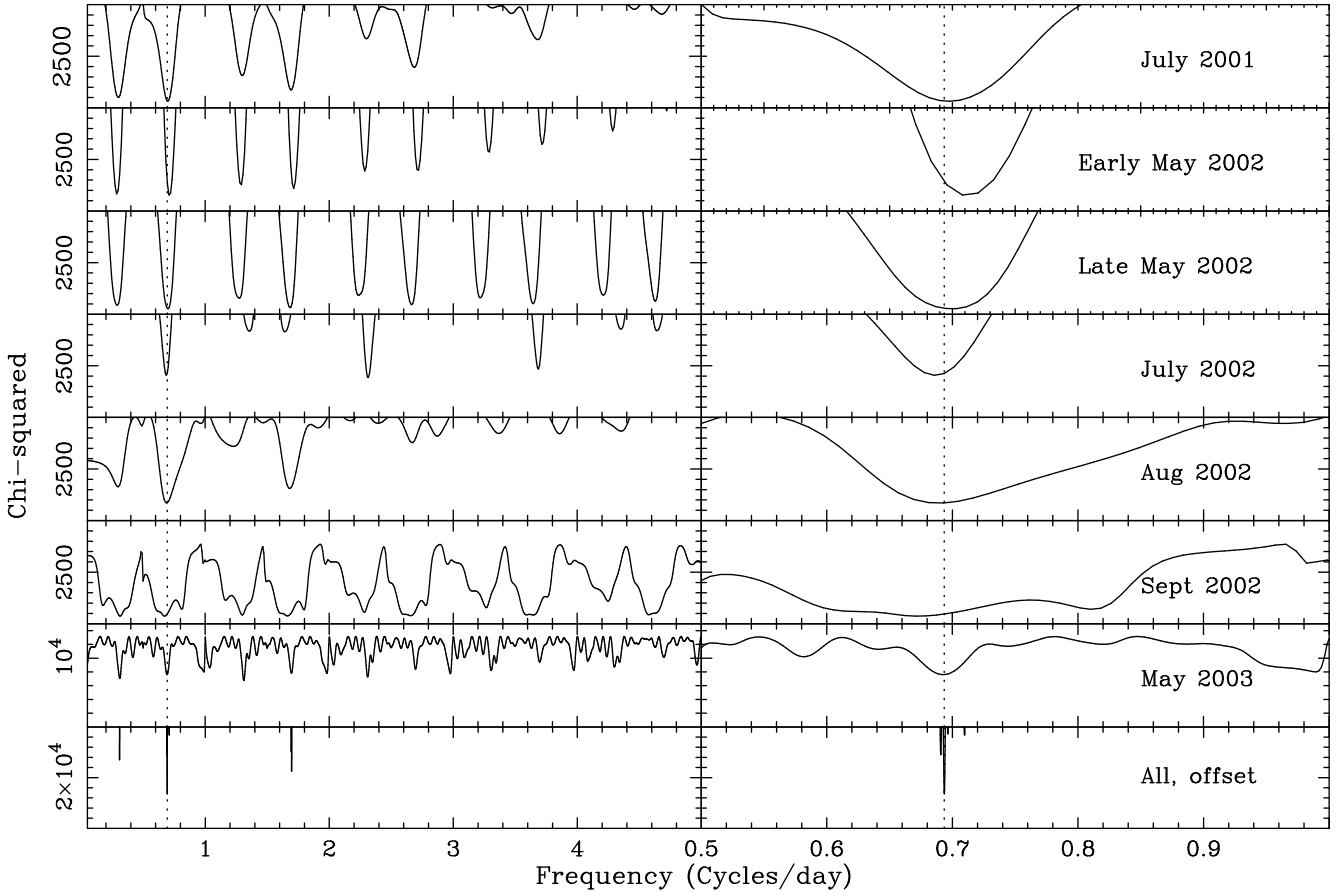


Figure 2. Periodograms for all of the 7 data sets. A period of approximately 1.4418 days is favoured (vertical dotted line). The expanded plots seem to show a slight shift in the best-fitting period (see Fig 4 and Section 4.2).

time than the edges. This was potentially important as the variation we were trying to measure between the target and comparisons was small - of order 2%. The flats were checked by dividing those of different exposure time by each other, and we found a gradient peaking in the centre of the chip. However, this effect was only seen in the September 2002 data, and was not only confined to the very low exposure times (< 2 s) as we were expecting, but affected flats with exposures of up to 20s. We suspect that this was caused by a loose filter moving with respect to the chip, but that these variations smoothed out over long exposure times. We therefore only used flats with exposure times of > 20 s to generate the master flat.

A single master flat was generated for each run in an attempt to remove systematic variations from night to night. This was not possible for the July 2001 run, as the first night's data was taken on a different part of the chip to the rest of the run, and there were no full-frame flats. Therefore the first night of that run is flatfielded with a different master flat to the other 6 nights. The first May 2002 run was flat fielded with dome flats as there were no sky flats available. All of the dome flats had exposure times of 10 seconds. The second May 2002 run had target frames with a mixture of fast and slow readout speeds. We therefore used two different master flats, one for the fast readout frames

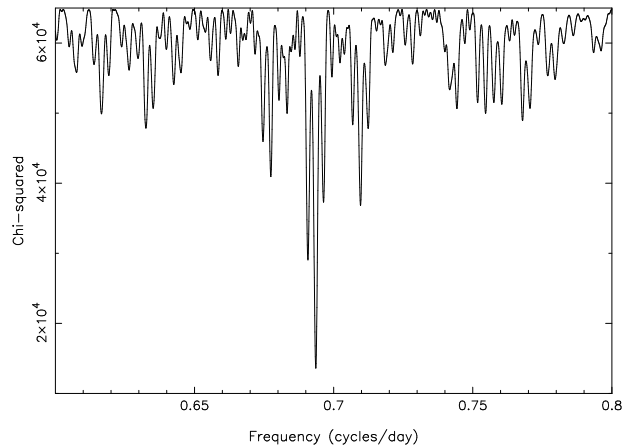


Figure 3. Periodogram zoomed in on the best-fitting period of 1.44176 days (0.6935 cycles/day).

and one for the slow. The May 2003 run was during a very dusty period, hence the flats changed nightly. This run was therefore flatfielded with an individual master flat for every night.

Once the master flats had been divided from the tar-

get frames, we performed aperture photometry using AUTOPHOTOM. This was performed with several different apertures to determine the optimum aperture radius of 4 pixels. The sky background was taken from an annulus around the target stars, the measurement errors were estimated from sky variance and the sky background level was estimated using the clipped mean of the pixel values in the annulus.

Results were output in counts. Once we had established that the three comparison stars were not varying, we combined their fluxes to give us one bright comparison star, and divided the target photometry by the newly generated comparison star to give us differential photometry of the target.

The July 2001 data had been taken with the Kitt Peak V filter, while the rest of the data was taken with the Harris V filter. We corrected for this by integrating models for a cool WD (for the target) and a G-type MS star (for the comparisons) through both filter responses, and multiplying the July 2001 data by the ratio. The correction to the differential photometry only amounted to a factor of 0.9974.

All times were corrected to heliocentric Julian days.

4 ANALYSIS AND RESULTS

4.1 Determining the periods

We used a “floating mean” periodogram (e.g. Cumming, Marcy & Butler, 1999; Morales-Rueda et al. 2003) to determine the period of each epoch separately, and all of the data together. This is a generalisation of the Lomb-Scargle periodogram (Lomb, 1976; Scargle, 1982) and involves fitting the data with a sinusoid plus constant of the form:

$$A + B \sin[2\pi f(t - t_0)],$$

where f is the frequency and t is the observation time. The advantage over the Lomb-Scargle periodogram is that it treats the constant, A , as an extra free parameter rather than fixing the zero-point and then fitting a sinusoid, i.e. it allows the zero-point to “float” during the fit. The resultant periodogram is an inverted χ^2 plot of the fit at each frequency (Figs 2 & 3).

4.2 Uncertainties in the periods

The errors output by the packages are the formal statistical errors, but due to the high signal to noise they are likely to be underestimates of the actual errors due to e.g. anomalies in the flat fields, aperture edge effects, and so on. We therefore obtained an independent estimate of our errors by bootstrapping our data. We fit the data for each epoch with a sine wave, then resampled the data, randomly selecting the same number of points and re-fitting with the sine wave (Diaconis & Efron, 1983). This was repeated 500000 times. The resultant period distributions can be seen in Fig 5. In order to avoid excessive weighting of a few data points, the errors were set to a standard average value before bootstrapping. The bootstrapping seems to indicate that there is a small change in the best-fitting period between each epoch. To test the robustness of this result to night-to-night systematic shifts we repeated the bootstrap runs after adding offsets to

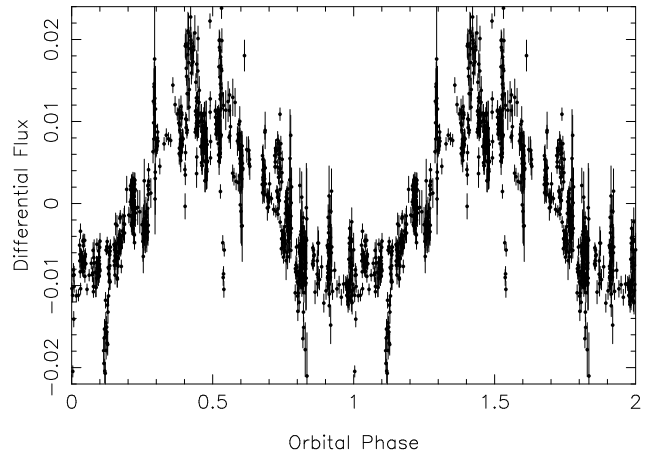


Figure 4. All of the data folded on the best-fitting period of 1.44176 days.

each night. The offsets were added as Gaussian random variables. We found that an RMS offset of only 0.003 magnitudes caused enough of a spread in the period distributions that the period shift between each epoch was no longer significant. As such a shift could be caused by anomalies in the flat fields, irregularities in the chip or by slight variations in the standard stars, we conclude that there is no evidence for a period change in WD1953-011 in our data.

The phase-folded light curve (Fig 4) shows a variation in the flux of $\pm 1\%$. Fig 2 shows the periodograms for each epoch, showing that the deepest minimum in χ^2 for all but one data set, and the only minimum common to all epochs, is that at approximately 0.69 cycles per day, corresponding to:

$$HJD = 2452489.3588(9) + 1.441769(8)E$$

which specifies the time of minimum light. The zero-point was selected to give the minimum correlation between it and the fitted period. The light curve also appears to be slightly non-sinusoidal at the level of 1-2 mmag in the 1st harmonic. There initially appear to be several sharp features in the folded light curve, most notably at phase 0.4. However, all of these outlying points are from single nights during either the first May 2002 or the July 2002 run. As these features are not seen at any of the other epochs, we believe that they are not significant features in the WD1953-011 light curve.

5 DISCUSSION AND CONCLUSIONS

The variation in the flux from WD1953-011 could be explained if it were a binary system, with the secondary emitting re-processed light visible for part of the orbital cycle. However, radial velocity measurements by Maxted et al. (2000) found that it was stable to within 2 km/s. Within this error, and using an orbital period of 1.44 days, it is still possible to miss a companion body with mass $< 0.009M_{\odot}$ ($\sim 10M_J$) orbiting at approximately 0.02 AU. However, as the WD is so cool with a relatively low UV flux, such a body would only re-process $\sim 0.013\%$ of the light from the white dwarf, and hence could not produce the variability on the $\sim 2\%$ peak-to-peak level that we see. This leads us to

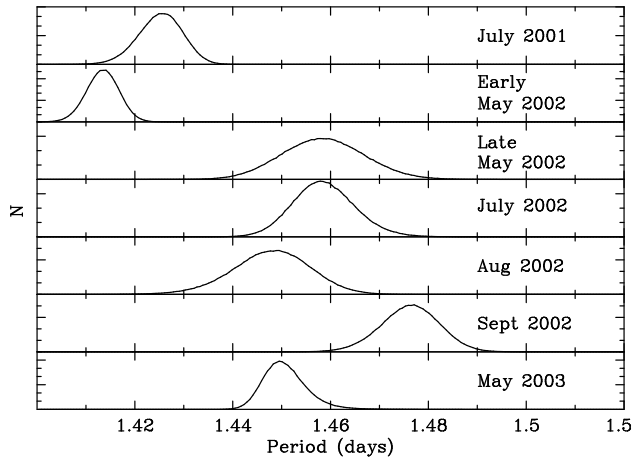


Figure 5. Period distributions for all 7 data sets after bootstrapping 500000 times and plotting over 200 bins (see Section 4.2).

believe that the variability is somehow caused by the magnetic field of the MWD. Periodic photometric variation has been seen before in white dwarfs with a high magnetic field strength, such as RE J0317-853 (Barstow et al. 1995). In these cases the variation is thought to be due to the field dependence of the continuum opacity (magnetic dichroism, Ferrario et al. 1997), but the field strength of WD1953-011 (~ 70 kG) is not large enough to cause this effect. Instead we believe that the variations may be caused by a star spot on the surface of the WD, analogous to a sun spot. Star spots occur when the atmospheric convection of the stellar atmosphere is inhibited by the magnetic field at the surface, so causing a spot of lower temperature, and therefore lower luminosity, to be formed. As the MWD rotates, the visibility of this cooler spot will vary, causing a periodic variation in the flux from the star. At a temperature of only ~ 7900 K, WD1953-011 is well below the limit required for a convective atmosphere (15000 K, Bergeron, Wesemael & Beauchamp, 1995), and therefore may be capable of forming star spots.

The visibility of the spot will depend upon the angle between the spin axis and our line of sight. Consider a small spot at latitude β on the white dwarf. The variation in the light curve will mainly depend upon the varying projected area of the spot as the white dwarf rotates (we ignore limb darkening as a second order effect).

Defining phase $\phi=0$ as the point at which spot is closest to us, then the cosine of the angle between the normal to the surface of the white dwarf at the location of the spot and our line of sight (α) is given by

$$\cos \alpha = \cos \beta \sin i \cos \phi + \cos i \sin \beta,$$

where i is the inclination of the spin axis to our line of sight. The projected area factor, $\cos \alpha$, therefore varies sinusoidally with the phase ϕ . This will be true so long as $\cos \alpha > 0$ for all ϕ (if $\cos \alpha < 0$ then the spot is not visible, so the light curve will be flat).

Therefore, for a sinusoidally varying light curve, we require that $\beta > i$. If seen at large i then the spot must be near the pole, but if i is small, then the spot could be almost anywhere on the visible hemisphere - the only condition is that $\beta > i$.

The amplitude of the light curve depends upon the size of the spot and how dark it is, and it would be easy to fit the

light curve for a variety of spot sizes. Since a spot of finite size is simply the result of integrating many infinitesimal spots, large spots can also lead to sinusoidal variations as long as every part of them satisfies the $\beta > i$ constraint. This is consistent with the model proposed by Maxted et al. (2000), who suggested that the magnetic spot may cover $\sim 10\%$ of the surface of the WD. Limb-darkening of the form $I \propto 1 - \epsilon + \epsilon \cos \alpha$ will introduce a first harmonic from the $\epsilon \cos \alpha$ factor. This will be negligible as long as

$$\frac{1}{2} \epsilon \cos \beta \sin i \ll 1 - \epsilon,$$

where ϵ is the linear limb-darkening coefficient. Taking $\epsilon \approx 0.6$, we require $\cos \beta \sin i \ll 1.3$. This can be satisfied along with $\beta > i$ by many values of spin axis inclination and spot latitude, e.g. $i = 30$, $\beta = 70$ gives $\cos \beta \sin i = 0.17$. In this case, a large spot would help suppress the harmonic term relative to the fundamental. Thus a spot on the surface provides a natural explanation for the sinusoidal flux variation that we see.

It has been suggested that the observed variations may be caused instead by the presence of circumstellar matter caught in the magnetic field of the WD as observed in some helium-rich Bp stars (e.g. Groote & Hunger, 1982). We believe that this is highly unlikely due to the absence of emission lines in the spectra of the star taken by Maxted et al. (2000), and the absence of a formation mechanism for these clouds. Three possible origins are suggested in Groote & Hunger (1982): that the clouds are left over matter from the formation of the WD; that they are formed through accreted matter; or that they are formed from mass lost by the WD. The first scenario is unlikely as any matter left over from the formation of the WD should have been driven off by radiation pressure while the WD was still very hot. Similarly, the second mechanism should produce emission lines in the MWD spectrum that are not seen in the observed spectra. Finally, the low temperature and low magnetic field strength of WD1953-011 make it doubtful that the stellar wind would be strong enough to drive mass loss from the WD, or that the ejected mass would be trapped by the field lines. We therefore find it improbable that the variations seen in WD1953-011 are caused by anything other than a feature on the surface of the WD itself.

6 ACKNOWLEDGEMENTS

CSB and SG acknowledge the support of PPARC studentships. TRM, LMR and MRB also acknowledge the support of PPARC. The Jacobus Kapteyn Telescope is operated on the island of La Palma by the Isaac Newton Group in the Spanish Observatorio del Roque de los Muchachos of the Instituto de Astrofísica de Canarias. This research has made use of the SIMBAD database, operated at CDS, Strasbourg, France.

REFERENCES

- Barstow M.A., Jordan S., O'Donoghue D., Burleigh M.R., Napiwotski R., Harrop-Allin M.K., 1995, MNRAS, 277, 971
- Bergeron P., Leggett S.K., Ruiz M.T., 2001, ApJS, 133, 413
- Bergeron P., Wesemael F. Beauchamp A., 1995, PASP, 107, 1047

- Cumming A., Marcy G.W., Butler R.P., 1999, *ApJ*, 526, 890
Diaconis P., Efron B., 1983, *Sci. Am.*, 248, No. 6, 96
Ferrario L., Vennes S., Wickramasinghe D.T., Bailey J., Christian D.J., 1997, *MNRAS*, 292, 205
Groote, D., & Hunger, K., 1982, *A&A*, 116, 64
Heber U., Napiwotski R., Reid I.N., 1997, *A&A*, 323, 819
King A.R., Pringle J.E., Wickramasinghe D.T., 2001, *MNRAS*, 320, L45
Maxted P.F.L., Ferrario L., Marsh T.R., Wickramasinghe D.T., 2000, *MNRAS*, 315, L41
Lomb N.R., 1976, *Ap&SS*, 39, 447
Morales-Rueda L., Maxted P.F.L., Marsh T.R., North R.C., Heber U., 2003, *MNRAS*, 338, 752
O'Brien M.S., Clemens J.C., Kawaler S.D., Dehner B.T., 1996, *ApJ*, 467, 397
Scargle J.D., 1982, *ApJ*, 263, 835
Spruit H.C., 1998, *A&A*, 333, 603
Wickramasinghe D.T., Ferrario L., 2000, *PASP*, 112, 873